Quasiparticle Energies and Band Gaps in Graphene Nanoribbons

Li Yang,[1,2] Cheol-Hwan Park,[1,2] Young-Woo Son,[3] Marvin L. Cohen,[1,2] and Steven G. Louie[1,2]

[1]*Department of Physics, University of California at Berkeley, California 94720, USA*
[2]*Materials Sciences Division, Lawrence Berkeley National Laboratory, Berkeley, California 94720, USA*
[3]*Department of Physics, Konkuk University, Seoul 143-701, Korea*

(Received 8 June 2007; published 1 November 2007)

We present calculations of the quasiparticle energies and band gaps of graphene nanoribbons (GNRs) carried out using a first-principles many-electron Green's function approach within the *GW* approximation. Because of the quasi-one-dimensional nature of a GNR, electron-electron interaction effects due to the enhanced screened Coulomb interaction and confinement geometry greatly influence the quasiparticle band gap. Compared with previous tight-binding and density functional theory studies, our calculated quasiparticle band gaps show significant self-energy corrections for both armchair and zigzag GNRs, in the range of 0.5–3.0 eV for ribbons of width 2.4–0.4 nm. The quasiparticle band gaps found here suggest that use of GNRs for electronic device components in ambient conditions may be viable.

DOI: 10.1103/PhysRevLett.99.186801 PACS numbers: 73.22.−f, 72.80.Rj, 75.70.Ak

Graphene, a single atomic layer of graphite, has been successfully produced in experiment [1–3], which has resulted in intensive investigations on graphene-based structures because of fundamental physics interests and promising applications [4–10]. When graphene is etched or patterned along one specific direction, a novel quasi-one-dimensional structure, a strip of graphene of nanometers in width, can be obtained, which is referred to as a graphene nanoribbon (GNR). The GNRs are predicted to exhibit various remarkable properties and may be a potential elementary structure for future carbon-based nanoelectronics [11–14]. In particular, as a fundamental factor in determining transport and optical properties, the electronic band structure of GNRs has been the subject of great interest.

Depending on specific GNRs, previous studies using tight-binding or massless Dirac fermion equation approaches have predicted GNRs to be either metals or semiconductors [15–20], whereas density functional theory (DFT) calculation showed that all zigzag-edged and armchair-edged GNRs have a finite band gap when relaxation of the structure or spin polarization is considered [13,21]. Recent experiments have reported finite band gaps in all the GNRs that have been tested [22,23]. However, it is well established [24] that the Kohn-Sham eigenvalues from DFT calculation are inappropriate to describe the band gaps of semiconductors. The disagreement between the Kohn-Sham band gap and experimental data is worse for nanostructures because of the enhanced electron-electron interaction in those systems. On the other hand, first-principles calculation based on many-body perturbation theory, such as the *GW* approximation [24,25], has been shown to be reliable for obtaining quasiparticle band gaps of nanosized semiconductors [26–29]. Motivated by the importance but the lack of accurate knowledge about quasiparticle band gaps of the GNRs and by the successes of the *GW* approximation for nanosize semiconductors, we carry out a first-principles calculation using the *GW* approximation to determine the quasiparticle energy spectrum and the band gaps of the GNRs.

We consider two common types of GNRs. Their structures are shown in Fig. 1. The left one, called armchair GNR (AGNR), has armchair-shaped edges; the right one, called zigzag GNR (ZGNR), has zigzag-shaped edges. The dangling σ bonds at the edges are passivated by hydrogen atoms. The structures of the GNRs studied here are fully relaxed according to the forces and stress on the atoms using local (spin) density approximation [L(S)DA]. Following conventional notation, a GNR is specified by the number of dimer lines or zigzag chains along the ribbon forming the width, for the AGNR and ZGNR, respectively, as explained in Fig. 1. For example, the structure of Fig. 1(a) is referred as a 11-AGNR and the structure in Fig. 1(b) as a 6-ZGNR. In addition, when referring to the width of a GNR here, we define the width without including the hydrogen atoms at the edge, as shown in Fig. 1.

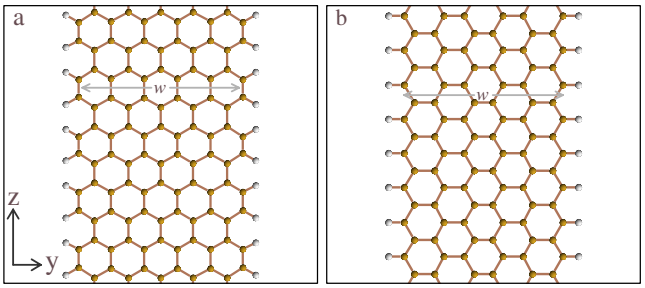

FIG. 1 (color online). (a) A ball-stick model for an 11-AGNR which has 11 C-C dimer lines making up its width w. Hydrogen atoms (white balls) are used to passivate the edge σ-dangling bonds. x, y, and z are the Cartesian coordinates, and the x axis is out of plane. (b) A ball-stick model for a 6-ZGNR which has 6 zigzag chains along the z direction.

Following the approach of Hybertsen and Louie [25], we first obtain the electronic ground state with DFT within the L(S)DA. Norm-conserving pseudopotentials [30] and the plane-wave basis are used with a 60 Ry energy cutoff. Then, the quasiparticle energies are calculated within the G_0W_0 approximation to the electron self-energy. The static dielectric matrix is calculated with an 8.0 Ry energy cutoff with the plane-wave basis and extended to finite frequencies with the generalized plasmon-pole model. To assure that the quasiparticle energies are converged to within 0.1 eV, a $1 \times 1 \times 32$ k-point sampling is used for AGNRs and a $1 \times 1 \times 64$ k-point sampling for ZGNRs. Since the supercell method is used in this calculation to mimic isolated GNRs, we use a truncated Coulomb interaction to eliminate the image effect between adjacent supercells [31–33]. Considering the geometry of the ribbons, we employ a rectangular-shape Coulomb truncation as

$$V_c = \frac{1}{r}\theta(|x| - x_c)\theta(|y| - y_c)\theta(|z| - z_c), \qquad (1)$$

where $r = \sqrt{x^2 + y^2 + z^2}$ is the distance between two electrons; x_c, y_c, and z_c are cutoff parameters. As discussed in previous studies [31], the dimension of the unit cell has to be $2x_c \times 2y_c \times 2z_c$. Because of the single layer structure of GNRs, the truncation lengths x_c and z_c are fixed for all GNRs in our calculations. The unit cell volume is linearly dependent on the width of a GNR, and the number of plane waves needed is also scaled linearly with the width of ribbon, which significantly reduces the cost of the computation. The spin degree of freedom is included in the GW calculations of ZGNRs, and the details can be found in Ref. [34].

The LDA and quasiparticle band gaps of 11 armchair GNRs are shown in Fig. 2. As is found in the LDA, the quasiparticle band structure has a direct band gap at the zone center for all AGNRs studied. In addition, the band gaps of the three families of n-AGNRs, which are classified according to whether $n = 3p + 1$, $3p + 2$, or $3p$ (n is the number of dimer chains as explained in Fig. 1, and p is an integer), show qualitatively the same hierarchy as those obtained in LDA ($E_g^{3p+1} > E_g^{3p} > E_g^{3p+2} \neq 0$).

However, the GW self-energy corrections to the band gap, E_g, are significant for all the AGNRs. The corrections are from 0.5 to 3 eV for the AGNRs in Fig. 2 with width from 1.6 to 0.4 nm, which are much larger than those found for bulk graphite or diamond [25]. A weaker screening contributes to this enhanced self-energy correction because the GNRs are isolated and surrounded by vacuum that does not screen the Coulomb interaction. In addition, the confined geometry (one-dimensional nature) of the GNRs enhances the effect of electron-electron interaction, which further enlarges the self-energy correction. This kind of enhanced self-energy correction is also found in other nanostructures such as nanotubes and nanowires [26–29].

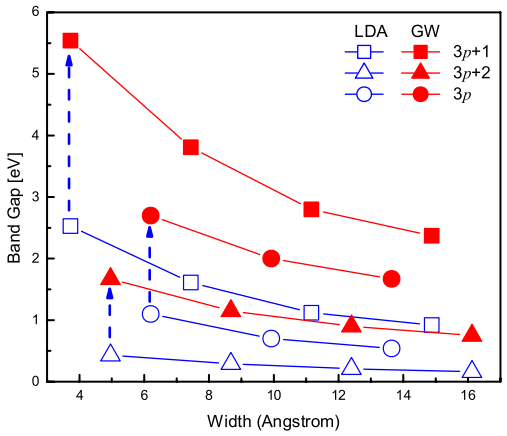

FIG. 2 (color online). Variation of band gaps with the width of AGNRs. The three families of AGNRs are represented by different symbols. The values of the same family of AGNRs are connected by solid lines as guides to the eyes. The open symbols are LDA band gaps while the solid symbols are the corresponding quasiparticle band gaps. Dashed arrows are used to indicate the self-energy correction for the smallest width ribbon of each of the three families of AGNRs studied.

The band gaps from both the LDA and GW calculations clearly show size dependence in Fig. 2 because of quantum confinement. Under a hard-wall boundary condition used in previous works, an inverse relation, $E_g \propto 1/(w + w_0)$, is widely applied to characterize the size dependence of the band gap in AGNRs, where w is the width defined in Fig. 2 and w_0 is a small constant (2.4 Å). This size dependence of the band gaps describes the tight-binding and LDA results well [21]. However, the boundary condition for the GNRs is not strictly a hard-wall condition, and the electron distribution will leak out of the boundary more or less. Therefore, the effective width of GNRs should be larger than the physical width w. Considering this effect, we use the formula

$$E_g = \frac{a}{w + w_0 + \delta}, \qquad (2)$$

to fit the band gap values in Fig. 2, and the fitted results are given in Table I. For LDA results, the parameter δ is close to zero or a little bit negative. For GW results, the parameter δ found is around 1.5 to 2.9 Å.

Figures 3(a) and 3(b) show the LSDA and quasiparticle band structure of 12-ZGNR. As predicted by previous works [21,35], the LSDA result of ZGNRs shows an anti-

TABLE I. Fitted parameters for the LDA and GW band gaps of AGNRs according to formula (2).

	LDA		GW	
Family	a(eV Å)	δ(Å)	a(eV Å)	δ(Å)
$3p + 1$	15.8	0.1	44.4	1.8
$3p + 2$	3.0	−0.4	14.6	1.3
$3p$	7.6	−1.7	31.3	2.9

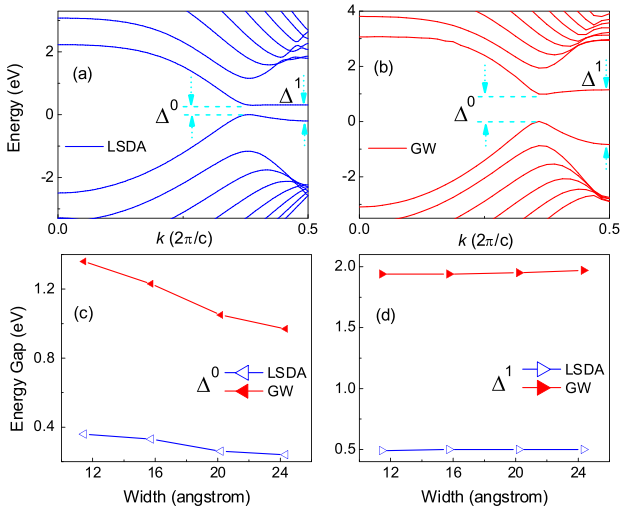

FIG. 3 (color online). Calculated band structure and energy gap of ZGNRs. (a) The LSDA band structure of a 12-ZGNR. The up and down spin states are degenerated for all the bands, and the top of the valence band is set at zero. The symbols, Δ^0 and Δ^1 denote the direct band gap and the energy gap at the zone boundary. (b) The quasiparticle band structure of a 12-ZGNR. (c) Variation of direct band gap with the width of ZGNRs. The open symbols denote the LSDA results while the solid symbols are the *GW* results. (d) Variation of the energy gap at the zone boundary with the width of ZGNRs. The symbols have the same meaning as those in (c).

ferromagnetic insulating ground state with ferromagnetic coupling at each zigzag edge and antiferromagnetic coupling across the ribbon. There are two notable characteristics in the electronic structure of ZGNRs: (1) the top of the valence band and the bottom of the conduction band are composed of mainly edge states; and (2) the spin interaction introduces a finite band gap in the ZGNRs. As shown in Figs. 3(c) and 3(d), the magnitudes of the self-energy corrections to the LSDA energy gaps in ZGNRs are similar to those in AGNRs, and the corrections enlarge the band gap by 0.8 to 1.5 eV for the ribbons studied. The spin polarization changes the screening type of ZGNRs from that of a metal to that of a semiconductor. Therefore, a significant self-energy correction results. We try to fit the width dependence of the quasiparticle band gaps in Fig. 3(c) with a functional form of $1/(w + \delta)$. The fitted δ of LSDA is almost zero, and it is 16 Å for the *GW* values, which is much larger than that in AGNRs. This is not unexpected, because it is the spin interaction between electrons close to the edge that induces the finite band gap in ZGNRs. Therefore, we do not expect a simple quantum-confinement effect, a $1/w$ size dependence of the band gap, in such narrow ZGNRs.

Unlike the band gap (Δ^0) located around three-fourths of the way to the Brillouin zone edge [Figs. 3(a) and 3(b)], the energy gap at the zone boundary (Δ^1) is not sensitive to the width of ZGNRs as seen in Fig. 3(d). Previous tight-binding calculations [35] show that the profile of edge states decays to the center of ZGNRs with the factor of e^{-ar}, where $a = -(2/\sqrt{3}c)\ln|2\cos\frac{kc}{2}|$ ($\frac{2\pi}{3} \leq kc \leq \pi$, c is the lattice constant of ZGNRs along the z direction). As a result, the band edge states close to the zone boundary are highly confined at the edge of ZGNRs. Because of their dominant edge-state character, these states are not sensitive to the width of the ribbons; hence, the gap Δ^1 is virtually independent of width.

Since the electronic wave function of the edge states is more and more confined to an edge of a ZGNR when its wave vector k approaches the zone boundary, it provides a possibility to see how the self-energy correction evolves with the localization of the electronic state. We plot the charge distributions of three electronic states of the first conduction band with different wave vector k and their corresponding self-energy correction values defined as E^{QP}-E^{LSDA} in Fig. 4. It is clear that the self-energy correction is enhanced when the state is confined at the edge as shown from Figs. 4(b) and 4(d). Because of the $1/r$ nature of the Coulomb interaction, the self-energy of a state is sensitive to the localization of the wave function. Therefore, a larger self-energy correction is found to the more localized edge state. As a consequence, the dependence of the *GW* correction on the wave vector significantly changes the band dispersion in ZGNRs from that of LSDA calculations, which can be seen from Figs. 3(a) and 3(b). A smaller effective mass and better mobility for the carriers are expected in ZGNRs for the *GW* bands as compared to the LSDA ones. For example, the effective mass of holes (electrons) in the 12-ZGNR within LSDA is around $0.14m_0$ ($0.41m_0$), and the *GW* calculation decreases the value to around $0.07m_0$ ($0.21m_0$) (m_0 is the rest mass of the free electron).

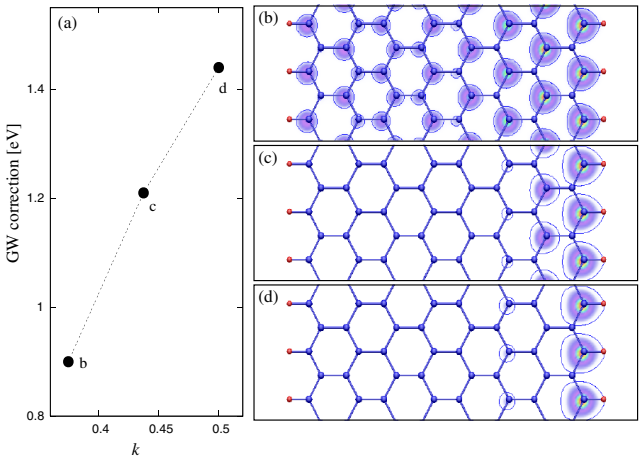

FIG. 4 (color online). (a) Variation of *GW* correction (the difference between the quasiparticle gap and the LSDA gap) with wave vector of electronic states ($k = 0.375$, 0.4375, and 0.50 in units of $2\pi/c$) in an 8-ZGNR. (b), (c), and (d) are the charge distributions of the conduction state with the corresponding wave vectors in (a). We plot the charge distribution of only one spin component because of the degeneracy of the up and down spin components.

Recently, several experiments related to the quasiparticle band gap in GNRs have been reported [22,23]. They have not only proven the existence of finite band gap in GNRs but also shown a larger gap when the width of the GNR decreases. Within a range of width of GNRs of 15 to 90 nm, a $E_g \propto 1/w$ relation is observed. This finding agrees qualitatively with our *GW* results. However, the experimental data are for the wider GNRs where the widths are far from the range of widths of our calculated GNRs (0.4–2.4 nm). In addition, all the GNRs in the experimental case are etched by the oxygen plasma, which could be different from our hydrogen-passivated GNRs. Therefore, it is difficult to compare our *GW* results with current experimental data directly. On the other hand, considering that the origin of the enhancement of the self-energy correction in GNRs is the quasi-one-dimensional geometry and weakened screening, we expect that other passivating atoms or molecules do not change the physics here significantly. With advances in experimental techniques, it is very possible that smaller-sized and hydrogen-passivated GNRs will soon be fabricated. A comparison between our first-principles results and experimental data can then be made.

In conclusion, we have performed a first-principles Green's function calculation within the *GW* approximation to obtain the quasiparticle band gaps in GNRs. Because of the enhanced electron-electron interaction in these quasi-one-dimensional systems, a significant self-energy correction is found for both armchair and zigzag GNRs. The quasiparticle energy of states near the band gap in ZGNRs is found to be wave vector sensitive, and this gives rise to a larger band width and smaller effective mass for carriers in ZGNRs. The calculated quasiparticle band gaps are within the most interesting range (1–3 eV for 2–1 nm GNRs) and give promise for applications of GNRs in nanoelectronics.

We thank F. Giustino, D. Prendergast, and E. Kioupakis for discussions. This research was supported by NSF Grant No. DMR04-39768 and by the Director, Office of Science, Office of Basic Energy under Contract No. DE-AC02-05CH11231. Y.-W. Son acknowledges support by the KOSEF grant funded by the MOST No. R01-2007-000-10654-0. Computational resources have been provided by Datastar at the San Diego Supercomputer Center.

[1] K. S. Novoselov *et al.*, Science **306**, 666 (2004).
[2] K. S. Novoselov *et al.*, Nature (London) **438**, 197 (2005).
[3] Y. Zhang, Y.-W. Tan, H. L. Stormer, and P. Kim, Nature (London) **438**, 201 (2005).
[4] K. S. Novoselov *et al.*, Proc. Natl. Acad. Sci. U.S.A. **102**, 10451 (2005).
[5] K. S. Novoselov, Z. Jiang, Y. Zhang, S. V. Morozov, H. L. Stormer, U. Zeitler, J. C. Maan, G. S. Boebinger, P. Kim, and A. K. Geim, Science **315**, 1379 (2007).
[6] Y. Zhang *et al.*, Appl. Phys. Lett. **86**, 073104 (2005).
[7] C. Berger *et al.*, J. Phys. Chem. B **108**, 19912 (2004).
[8] N. M. R. Peres, F. Guinea, and A. H. Castro Neto, Phys. Rev. B **73**, 125411 (2006).
[9] C. L. Kane and E. J. Mele, Phys. Rev. Lett. **95**, 226801 (2005).
[10] V. M. Pereira *et al.*, Phys. Rev. Lett. **96**, 036801 (2006).
[11] Y.-W. Son, M. L. Cohen, and S. G. Louie, Nature (London) **444**, 347 (2006).
[12] K. Wakabayashi, Phys. Rev. B **64**, 125428 (2001).
[13] V. Barone, O. Hod, and G. E. Scuseria, Nano Lett. **6**, 2748 (2006).
[14] D. A. Areshkin, D. Gunlycke, and C. T. White, Nano Lett. **7**, 204 (2007).
[15] K. Nakada, M. Fujita, G. Dresselhaus, and M. S. Dresselhaus, Phys. Rev. B **54**, 17954 (1996).
[16] K. Wakabayashi, M. Fujita, H. Ajiki, and M. Sigrist, Phys. Rev. B **59**, 8271 (1999).
[17] M. Ezawa, Phys. Rev. B **73**, 045432 (2006).
[18] L. Brey and H. A. Fertig, Phys. Rev. B **73**, 235411 (2006).
[19] K.-I. Sasaki, S. Murakami, and R. Saito, J. Phys. Soc. Jpn. **75**, 074713 (2006).
[20] D. A. Abanin, P. A. Lee, and L. S. Levitov, Phys. Rev. Lett. **96**, 176803 (2006).
[21] Y.-W. Son, M. L. Cohen, and S. G. Louie, Phys. Rev. Lett. **97**, 216803 (2006).
[22] Z. Chen, Y.-M. Lin, M. J. Rooks, and P. Avouris, arXiv:cond-mat/0701599v1.
[23] M. Y. Han, B. Oezyilmaz, Y. Zhang, and P. Kim, Phys. Rev. Lett. **98**, 206805 (2007).
[24] S. G. Louie, *Conceptual Foundations of Materials: A Standard Model for Ground- and Excited-State Properties; Contemporary Concepts of Condensed Matter Science* (Elsevier, New York, 2006).
[25] M. S. Hybertsen and S. G. Louie, Phys. Rev. B **34**, 5390 (1986).
[26] C. D. Spataru, S. Ismail-Beigi, L. X. Benedict, and Steven G. Louie, Phys. Rev. Lett. **92**, 077402 (2004).
[27] X. Y. Zhao, C. M. Wei, L. Yang, and M. Y. Chou, Phys. Rev. Lett. **92**, 236805 (2004).
[28] L. Wirtz, A. Marini, and A. Rubio, Phys. Rev. Lett. **96**, 126104 (2006).
[29] C.-H. Park, C. D. Spataru, and S. G. Louie, Phys. Rev. Lett. **96**, 126105 (2006).
[30] N. Troullier and J. L. Martins, Phys. Rev. B **43**, 1993 (1991).
[31] C. D. Spataru, S. Ismail-Beigi, L. X. Benedict, and S. G. Louie, Appl. Phys. A: Mater. Sci. Process. **78**, 1129 (2004).
[32] S. Ismail-Beigi, Phys. Rev. B **73**, 233103 (2006).
[33] C. A. Rozzi, D. Varsano, A. Marini, E. K. U. Gross, and A. Rubio, Phys. Rev. B **73**, 205119 (2006).
[34] J.-L. Li, G.-M. Rignanese, E. K. Chang, X. Blase, and Steven G. Louie, Phys. Rev. B **66**, 035102 (2002).
[35] M. Fujita, K. Wakabayashi, K. Nakada, and K. Kusakabe, J. Phys. Soc. Jpn. **65**, 1920 (1996).